Eur. Phys. J. C 22, 667–675 (2002)
Digital Object Identifier (DOI) 10.1007/s100520100843

THE EUROPEAN PHYSICAL JOURNAL C

Unitarity constraints and role of geometrical effects in deep-inelastic scattering and vector meson electroproduction

S.M. Troshin, N.E. Tyurin

Institute for High Energy Physics, Protvino, Moscow Region, 142280, Russia

Received: 10 September 2001 /
Published online: 7 December 2001 –

Abstract. Deep-inelastic scattering at low x and elastic vector meson electroproduction are analyzed on the basis of the s-channel unitarity extended to off-shell particle scattering. It appeared that the role of unitarity is important, but contrary to the case of on-shell scattering it does not rule out a power-like behavior of the total cross sections. We discuss the behavior of the total cross section of virtual photon–proton scattering in the geometrical approach and obtain the result that the exponent of the power-like energy dependence of $\sigma^{\rm tot}_{\gamma^* p}$ is related to the constituent quark interaction radius. The mass effects and energy dependence of vector meson electroproduction are discussed along with the angular distributions at large momentum transfers in these processes.

Introduction

The increasing dependence of the virtual photon–proton scattering total cross section on the center of mass energy W^2 discovered at HERA [1] led to renewed interest in the mechanism of diffraction at high energies. Such a behavior was in fact predicted in [2] and expected in perturbative QCD [3]. The total virtual photon–proton cross section is related to the structure function F_2 at small x. The HERA effect is consistent with various W^2-dependences of $\sigma^{\rm tot}_{\gamma^* p}$ and has been explained in different ways; among them is to take it as the manifestation of a hard BFKL pomeron [4], the appearance of DGLAP evolution in perturbative QCD [3], transient phenomena, i.e. pre-asymptotic effects [5] or a true asymptotical off-mass shell scattering amplitude behavior [6]. There is an extensive list of papers devoted to this subject and many interesting results are described in review papers (cf. e.g. [1,7]). The strong increase of the structure function F_2 at small x which can be described by a power-like dependence[1] $F_2(x,Q^2) \propto x^{-\lambda(Q^2)}$ implies that

$$\sigma^{\rm tot}_{\gamma^* p}(W^2,Q^2) \propto (W^2)^{\lambda(Q^2)}, \qquad (1)$$

with $\lambda(Q^2)$ increasing with Q^2 from about 0.1 to about 0.5, and this is regarded as a somewhat surprising fact. It is due to the fact that according to the experimental data on the energy dependence of the total cross sections in hadronic interactions, the total cross section increase is rather slow ($\lambda \sim 0.1$). The mentioned variance may be regarded to be not a fundamental one. First, there is no Froissart–Martin bound for the case of off-shell particles [2,6]. Additional assumptions are needed to reinstate this bound [11,12]. Second, it cannot be taken for granted that the pre-asymptotic effects and the approach to the asymptotics are the same for the on-shell and off-shell scattering. It seems that, for some reasons, scattering of virtual particles reaches the asymptotics faster than the scattering of the real particles.

It is worth noting that the space-time structure of the low-x scattering involves large distances $l \sim 1/mx$ on the light-cone [13], and the region of $x \sim 0$ is sensitive to non-perturbative contributions. Deep-inelastic scattering in this region turns out to be a coherent process, where diffraction plays a major role and non-perturbative models such as a Regge or vector dominance model can be competitive with perturbative QCD and successfully applied for the description of the experimental data.

It is essential to obey the general principles in the non-perturbative region and, in particular, to satisfy unitarity. The most common form of the unitarity solution – the eikonal one – was generalized for off-shell scattering in [6]. In this paper we consider an off-shell extension of the U-matrix approach to the amplitude unitarization. It is shown that this approach along with the respective extension of the quark model for the U-matrix [14] leads to (1), where the exponent $\lambda(Q^2)$ is related to the Q^2-dependent interaction radius attributed to the constituent

[1] The most recent results of the H1 Collaboration [8] confirmed an x-independence of the exponent λ at low x by measuring the derivative $\left(\partial \ln F_2(x,Q^2)/\partial \ln x\right)_{Q^2}$ as a function both of Q^2 and of x for the first time. Some provisions against this independence were mentioned in [9]; moreover, there are also other parameterizations which describe the experimental data equally well (cf. e.g. [10]). Despite that, it seems that the parameterization (1) provides the most natural way to approximate the available experimental data

quark. These results cannot be obtained in the eikonal unitarization which reproduces a bare "Born" input form with subleading corrections for the output amplitude in the case of off-shell scattering [6]. The fundamental distinction between the two forms of amplitude unitarization lies in the analytical properties in the complex energy plane [15].

It is worth noting the importance of the effective interaction radius concept [16]. The study of the effective interaction radius dependence on the scattering variables appeared to be very useful for understanding the dynamics of high energy hadronic reactions [17,18]. It is widely known nowadays that the respective geometrical considerations provide a deep insight in hadron dynamics and deep-inelastic scattering (cf. [19]).

Besides the studies of deep-inelastic scattering (DIS) at low x the measurements of the characteristics of the elastic vector meson (VM) production were performed in the H1 and ZEUS experiments at HERA [21,22]. It was shown that the integral cross section of the elastic vector meson production increases with energy in a way similar to the $\sigma^{\rm tot}_{\gamma^* p}(W^2, Q^2)$ dependence on W^2 [1]. It appeared that an increase of the VM electroproduction cross section with energy is steeper for heavier vector mesons as well as when the virtuality Q^2 is higher. A discussion of such a behavior in various model approaches based on non-perturbative hadron physics or perturbative QCD can be found in, e.g., [7].

The application of the approach based on the off-shell extension of the s-channel unitarity to elastic vector meson electroproduction $\gamma^* p \to Vp$ allows one to obtain the angular dependence and predict interesting mass effects in these processes. It appears that the obtained mass and Q^2 dependences do not contradict the experimentally observed trends. It is also valid for the angular distributions at large momentum transfers.

1 Off-shell unitarity

An extension of the U-matrix unitarization scheme for the off-shell scattering was considered briefly in [11]. Here we give a more detailed treatment of this problem. We adopt the commonly accepted picture of DIS at small x, i.e. it is supposed that the virtual photon fluctuates into a quark–antiquark pair $q\bar{q}$ and this pair is considered as an effective virtual vector meson state in processes with small x. This effective virtual meson then interacts with a hadron. For simplicity we consider a single effective vector meson field. We use for the amplitudes of the processes

$$V^* + h \to V^* + h, \quad V^* + h \to V + h \quad \text{and} \quad V + h \to V + h \tag{2}$$

the notation $F^{**}(s,t,Q^2)$, $F^*(s,t,Q^2)$ and $F(s,t)$, respectively, i.e. we denoted in that way the amplitudes when both initial and final mesons are off-mass shell, and only the initial meson is off-mass shell and both mesons are on-mass shell.

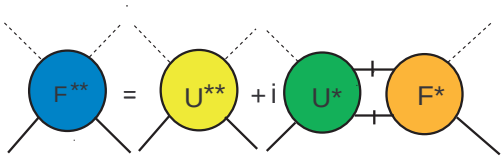

Fig. 1. The solution of the off-shell unitarity relation for the amplitude F^{**}

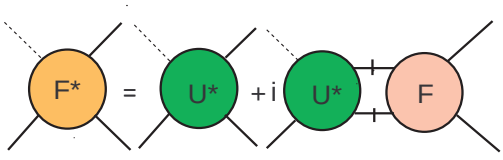

Fig. 2. The solution of the off-shell unitarity relation for the amplitude F^*

The unitarity relation for the amplitudes F^{**} and F^* has a similar structure as the unitarity equation for the on-shell amplitude F but relates, in fact, different amplitudes. Therefore, the unitarity constraints in DIS are much less stringent than in hadron–hadron scattering. In the impact parameter representation at high energies it relates the amplitudes F^{**} and F^* in the following way:

$$\mathrm{Im}F^{**}(s,b,Q^2) = |F^*(s,b,Q^2)|^2 + \eta^{**}(s,b,Q^2), \tag{3}$$

where $\eta^{**}(s,b,Q^2)$ is the contribution to the unitarity of many-particle intermediate on-shell states. The function $\eta^{**}(s,b,Q^2)$ is the sum of the n-particle production cross section in the process of the virtual meson interaction with a hadron h, i.e.

$$\eta^{**}(s,b,Q^2) = \sum_n \sigma_n(s,b,Q^2).$$

There is a similar relation for the functions F^* and F:

$$\mathrm{Im}F^*(s,b,Q^2) = F^*(s,b,Q^2)F(s,b,Q^2) + \eta^*(s,b,Q^2). \tag{4}$$

Contrary to $\eta^{**}(s,b,Q^2)$, the function $\eta^*(s,b,Q^2)$ has no simple physical meaning, and it will be discussed later. The solution of the off-shell unitarity relations are graphically represented for the amplitudes F^{**} and F^* in Figs. 1 and 2 respectively and has a simple form in the impact parameter representation:

$$\begin{aligned} F^{**}(s,b,Q^2) &= U^{**}(s,b,Q^2) \\ &\quad + \mathrm{i}U^*(s,b,Q^2)F^*(s,b,Q^2), \\ F^*(s,b,Q^2) &= U^*(s,b,Q^2) \\ &\quad + \mathrm{i}U^*(s,b,Q^2)F(s,b). \end{aligned} \tag{5}$$

It is worth noting that the solution of the off-shell unitarity in the non-relativistic case for a K-matrix representation was obtained for the first time in [23]. The solution of this system is

$$F^*(s,b,Q^2) = \frac{U^*(s,b,Q^2)}{1 - \mathrm{i}U(s,b)} = \frac{U^*(s,b,Q^2)}{U(s,b)}F(s,b), \tag{6}$$

$$
\begin{aligned}
&F^{**}(s,b,Q^2)\\
&=\frac{U^{**}(s,b,Q^2)}{1-\mathrm{i}U(s,b)}-\mathrm{i}\frac{U^{**}(s,b,Q^2)U(s,b)-[U^{*}(s,b,Q^2)]^2}{1-\mathrm{i}U(s,b)}\\
&=\frac{U^{**}(s,b,Q^2)}{U(s,b)}F(s,b)-\mathrm{i}U^{*}(s,b,Q^2)\\
&\quad\times\left[\frac{U^{**}(s,b,Q^2)}{U^{*}(s,b,Q^2)}-\frac{U^{*}(s,b,Q^2)}{U(s,b)}\right]F(s,b), \qquad (7)
\end{aligned}
$$

where the on-shell amplitude $F(s,b)$ has the following representation:

$$F(s,b)=U(s,b)/[1-\mathrm{i}U(s,b)]. \qquad (8)$$

We assume the following relation to be valid at the level of the "Born" amplitudes in the impact parameter space:

$$\frac{U^{*}}{U}=\frac{U^{**}}{U^{*}}. \qquad (9)$$

This relation is valid, e.g. in the Regge model with factorizable residues and Q^2-independent trajectory. It is also valid in the off-shell extension of the chiral quark model for the U-matrix which we will consider further. Equation (9) implies the following forms for the impact parameter dependent functions U^{*} and U^{**}:

$$
\begin{aligned}
U^{*}(s,b,Q^2)&=\omega(s,b,Q^2)U(s,b),\\
U^{**}(s,b,Q^2)&=\omega(s,b,Q^2)U(s,b)\omega(s,b,Q^2). \qquad (10)
\end{aligned}
$$

This factorization may be treated as a reflection of the universality of the initial and final state interactions responsible for the transitions between the on- and off-mass shell states. This seems to be a quite natural assumption. Note that this factorization does not survive for the amplitudes $F(s,t)$, $F^{*}(s,t,Q^2)$ and $F^{**}(s,t,Q^2)$, i.e. after a Fourier–Bessel transform is performed.

Thus, we have for the amplitudes F^{*} and F^{**} the following relations:

$$F^{*}(s,b,Q^2)=\frac{U^{*}(s,b,Q^2)}{1-\mathrm{i}U(s,b)}=\omega(s,b,Q^2)F(s,b), \qquad (11)$$

$$
\begin{aligned}
F^{**}(s,b,Q^2)&=\frac{U^{**}(s,b,Q^2)}{1-\mathrm{i}U(s,b)}\\
&=\omega(s,b,Q^2)F(s,b)\omega(s,b,Q^2), \qquad (12)
\end{aligned}
$$

and unitarity provides the inequalities

$$
\begin{aligned}
|F^{*}(s,b,Q^2)|&\le|\omega(s,b,Q^2)|,\\
|F^{**}(s,b,Q^2)|&\le|\omega^2(s,b,Q^2)|. \qquad (13)
\end{aligned}
$$

It is worth noting that the above limitations are much less stringent than the limitation for the on-shell amplitude $|F(s,b)|\le 1$. As a result, there is no Froissart–Martin bound in DIS at low x and the experimentally observed power-like energy dependence of the total cross section can represent a true asymptotical dependence.

When the function $\omega(s,b,Q^2)$ is real, we can write down a simple expression for the inelastic overlap function $\eta^{**}(s,b,Q^2)$:

$$\eta^{**}(s,b,Q^2)=\omega(s,b,Q^2)\frac{\mathrm{Im}U(s,b)}{|1-\mathrm{i}U(s,b)|^2}\omega(s,b,Q^2). \qquad (14)$$

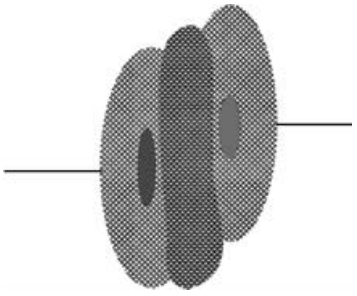

Fig. 3. Schematic view of initial stage of the hadron interaction and formation of the effective field

The following relation is valid for the function $\eta^{*}(s,b,Q^2)$:

$$\eta^{*}(s,b,Q^2)=[\eta^{**}(s,b,Q^2)\eta(s,b)]^{1/2}. \qquad (15)$$

Equation (15) allows one to connect the integral

$$\Sigma(s,Q^2)\equiv 8\pi\int_0^{\infty}\eta^{*}(s,b,Q^2)b\mathrm{d}b$$

with the total inelastic cross section:

$$\Sigma(s,Q^2)|_{Q^2\to 0}=\sigma_{\mathrm{inel}}(s).$$

2 Off-shell scattering and the quark model for the U-matrix

The above formulas are rather general and are not useful alone in an analysis of the data. We need an explicit form for the functions U, U^{*} and U^{**} and therefore a phenomenological model is to be constructed. As a starting point we use the quark model for the hadron scattering described in [14]. In this section we list the main features and then construct an off-shell extension of the model. In fact this is based on the ideas of chiral quark models. The picture of the hadron structure in the model with valence constituent quarks located in the central part and a surrounding condensate implies that the overlapping of hadron structures and the interaction of the condensates occur at the first stage of the collision and results in generation of the quasi-particles, i.e. massive quarks (cf. Fig. 3).

These quarks play the role of scatterers. To estimate the number of such quarks one could assume that part of the hadron energy carried by the outer condensate clouds is being released in the overlap region to generate massive quarks. Then their number can be estimated by the quantity

$$\tilde{N}(s,b)\propto\frac{(1-k_Q)\sqrt{s}}{m_Q}D_c^h\otimes D_c^V, \qquad (16)$$

where m_Q is the constituent quark mass, and k_Q the fraction hadron energy carried by the constituent valence quarks. The function D_c^h describes the condensate distribution inside the hadron h, and b is the impact parameter of the colliding hadron h and meson V. Thus, $\tilde{N}(s,b)$

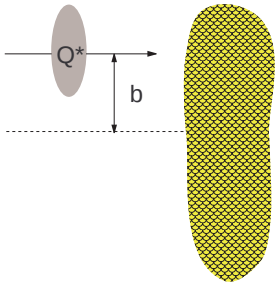

Fig. 4. Schematic view of the virtual constituent quark Q^* scattering in the effective field generated by $N_{\rm sc}(s,b)$ scatterers, where $N_{\rm sc}(s,b) = \tilde{N}(s,b) + N - 1$

quarks appear in addition to $N = n_h + n_V$ valence quarks. Those quarks are transient ones: they are transformed back into the condensates of the final hadrons in elastic scattering. It should be noted that we use the subscript Q to refer the constituent quark Q and the same letter Q is used to denote the virtuality Q^2. However, they enter formulas in a way excluding confusion.

In this model the valence quarks located in the central part of a hadron are supposed to scatter in a quasi-independent way by the effective field. Due to the quasi-independence of the valence quarks scatterings the basic dynamical quantity (the function U) can be factorized. When one of the hadrons (a vector meson in our case) is off-mass shell, the corresponding function $U^{**}(s,b,Q^2)$ is represented as the following product:

$$U^{**}(s,b,Q^2) = \prod_{i=1}^{n_h} \langle f_{Q_i}(s,b)\rangle \prod_{j=1}^{n_V} \langle f_{Q_j^*}(s,b,Q^2)\rangle. \quad (17)$$

The factors $\langle f_Q(s,b)\rangle$ and $\langle f_{Q^*}(s,b,Q^2)\rangle$ correspond to the individual quark scattering amplitudes smeared over the constituent quark transverse position and the fraction of longitudinal momentum carried by this quark. By the virtual constituent quarks Q^* we mean the ones composing the virtual meson. The factorization (17) reflects the coherence in the valence quark scattering, i.e. all valence quarks are scattered in the effective field simultaneously and there are no spectator valence quarks. This factorization might be considered as an effective implementation of the constituent quarks' confinement. The averaged amplitudes $\langle f_Q(s,b)\rangle$ and $\langle f_{Q^*}(s,b,Q^2)\rangle$ describe elastic scattering of single valence on-shell or off-shell quarks Q and Q^*, respectively, off the effective field (cf. Fig. 4). We use for the function $\langle f_Q(s,b)\rangle$ the following expression:

$$\langle f_Q(s,b)\rangle = [\tilde{N}(s,b) + (N-1)]V_Q(b), \quad (18)$$

where $V_Q(b)$ has the simple form

$$V_Q(b) \propto g\exp(-m_Q b/\xi),$$

which corresponds to the quark interaction radius

$$r_Q = \xi/m_Q.$$

The function $\langle f_Q^*(s,b,Q^2)\rangle$ is to be written

$$\langle f_{Q^*}(s,b,Q^2)\rangle = [\tilde{N}(s,b) + (N-1)]V_{Q^*}(b,Q^2). \quad (19)$$

In the above equation

$$V_{Q^*}(b,Q^2) \propto g(Q^2)\exp(-m_Q b/\xi(Q^2)), \quad (20)$$

and this form corresponds to the virtual constituent quark interaction radius

$$r_{Q^*} = \xi(Q^2)/m_Q. \quad (21)$$

The functions $V_Q(b)$ and $V_{Q^*}(b,Q^2)$ in the model are associated with the "matter" distribution inside constituent quarks and can be considered as strong formfactors.

Equations (18) and (19) imply that each valence quark is being scattered by all other $N-1$ valence quarks belonging to the same hadron as well as to the other hadron and by $\tilde{N}(s,b)$ quarks produced by the excitation of the chiral condensates. Due to the different radii the b-dependence of $\tilde{N}(s,b)$ being weak compared to the b-dependence of V_Q or V_{Q^*} and this function can be approximately taken to be independent on the impact parameter b. The dependence on the virtuality Q^2 comes through the dependence of the intensity of the virtual constituent quark interaction $g(Q^2)$ and the $\xi(Q^2)$, which determines the quark interaction radius (in the on-shell limit $g(Q^2) \to g$ and $\xi(Q^2) \to \xi$).

The introduction of the Q^2 dependence in the interaction radius of a constituent quark which in the present approach consists of a current quark and a cloud of quark–antiquark pairs of different flavors is the main issue of the off-shell extension of the model, and the origin of this dependence and its possible physical interpretation will be discussed in Sect. 6.

According to these considerations the explicit functional forms for the generalized reaction matrices U^* and U^{**} can easily be written in the form of (10) with

$$\omega(s,b,Q^2) = \frac{\langle f_{Q^*}(s,b,Q^2)\rangle}{\langle f_Q(s,b)\rangle}. \quad (22)$$

Note that (9) and (10) imply that the amplitude of the process $Q^* \to Q$ is

$$\langle f_{Q^*\to Q}(s,b,Q^2)\rangle = [\langle f_{Q^*}(s,b,Q^2)\rangle\langle f_Q(s,b)\rangle]^{1/2}.$$

We consider the high-energy limit and for simplicity assume here that all the constituent quarks have equal masses and the parameters g and ξ as well as $g(Q^2)$ and $\xi(Q^2)$ do not depend on quark flavor. We also assume pure imaginary amplitudes. Then the functions U, U^* and U^{**} are the following:

$$U(s,b) = {\rm i}g^N \left(\frac{s}{m_Q^2}\right)^{N/2} \exp\left[-\frac{m_Q N b}{\xi}\right], \quad (23)$$

$$U^*(s,b,Q^2) = \omega(b,Q^2)U(s,b),$$
$$U^{**}(s,b,Q^2) = \omega^2(b,Q^2)U(s,b), \quad (24)$$

where the function ω is energy independent and has the following dependence on b and Q^2:

$$\omega(b,Q^2) = \frac{g(Q^2)}{g}\exp\left[-\frac{m_Q b}{\bar{\xi}(Q^2)}\right], \quad (25)$$

with

$$\bar{\xi}(Q^2) = \frac{\xi\xi(Q^2)}{\xi - \xi(Q^2)}. \tag{26}$$

3 Total cross sections of $\gamma^* p$ interactions

With the explicit forms of the functions U, U^* and U^{**} the corresponding scattering amplitudes can be calculated. The most simple case is the forward scattering at large energies. For the on-shell scattering when $\omega \to 1$ at large W^2, the total photoproduction cross section has a Froissart-like asymptotic behavior

$$\sigma^{\rm tot}_{\gamma p}(W^2) \propto \frac{\xi^2}{m_Q^2} \ln^2 \frac{W^2}{m_Q^2}, \tag{27}$$

where the usual notation for DIS, W^2 instead of s, is used. A similar result is valid also for the off-mass shell particles if the interaction radius of virtual quark does not depend on Q^2 and is equal to the interaction radius of the on-shell quark, i.e. $\xi(Q^2) \equiv \xi$. The behavior of the total cross section at large W^2 is given by

$$\sigma^{\rm tot}_{\gamma^* p}(W^2) \propto \left[\frac{g(Q^2)\xi}{g m_Q}\right]^2 \ln^2 \frac{W^2}{m_Q^2}. \tag{28}$$

We consider next the off-shell scattering and suppose now that $\xi(Q^2) \neq \xi$. It should be noted first that for the case when $\xi(Q^2) < \xi$ the total cross section would be energy independent,

$$\sigma^{\rm tot}_{\gamma^* p}(W^2) \propto C(Q^2) \equiv \left[\frac{g(Q^2)\xi}{g\lambda(Q^2) m_Q}\right]^2,$$

in the asymptotic region. This scenario would mean that the experimentally observed increase of $\sigma^{\rm tot}_{\gamma^* p}$ is a transient pre-asymptotic phenomenon. This can be realized when we replace the mass m_Q by the quantity $m_{Q^*} = (m_Q^2 + Q^2)^{1/2}$ in order to obtain the interaction radius of the off-shell constituent quark and write it down as $r_{Q^*} = \xi/m_{Q^*}$, or equivalently replace ξ by $\xi(Q^2) = \xi m_Q/(m_Q^2 + Q^2)^{1/2}$. The above option cannot be excluded in principle; however, it is a self-consistent choice in the framework of the model only at large $Q^2 \gg m_Q^2$ since it was originally supposed that the function ξ is universal for the different quark flavors.

However, when $\xi(Q^2) > \xi$ the situation is different and we have at large W^2

$$\sigma^{\rm tot}_{\gamma^* p}(W^2, Q^2) \propto G(Q^2) \left(\frac{W^2}{m_Q^2}\right)^{\lambda(Q^2)} \ln \frac{W^2}{m_Q^2}, \tag{29}$$

where

$$\lambda(Q^2) = \frac{\xi(Q^2) - \xi}{\xi(Q^2)}. \tag{30}$$

We shall further concentrate on this self-consistent case for any Q^2 values and in the most interesting case.

All the above expressions for $\sigma^{\rm tot}_{\gamma^* p}(W^2)$ can be rewritten as the corresponding dependences of $F_2(x, Q^2)$ at small x according to the relation

$$F_2(x, Q^2) = \frac{Q^2}{4\pi^2\alpha} \sigma^{\rm tot}_{\gamma^* p}(W^2),$$

where $x = Q^2/W^2$.

In particular, (29) will appear in the form

$$F_2(x, Q^2) \propto \tilde{G}(Q^2) \left(\frac{1}{x}\right)^{\lambda(Q^2)} \ln(1/x). \tag{31}$$

It is interesting that the value and Q^2 dependence of the exponent $\lambda(Q^2)$ is related to the interaction radius of the virtual constituent quark. The value of the parameter ξ in the model is determined by the slope of the differential cross section of elastic scattering at large t [26], i.e.

$$\frac{{\rm d}\sigma}{{\rm d}t} \propto \exp\left[-\frac{2\pi\xi}{m_Q N}\sqrt{-t}\right], \tag{32}$$

and from the pp experimental data it follows that $\xi = 2$. Then from the data for $\lambda(Q^2)$ obtained at HERA [8] we can calculate the "experimental" Q^2-dependence of the function $\xi(Q^2)$:

$$\xi(Q^2) = \frac{\xi}{1 - \lambda(Q^2)}. \tag{33}$$

Evidently experiment indicates that $\xi(Q^2)$ increases with Q^2. This increase is slow and consistent with extrapolation of $\ln Q^2$ (Fig. 5):

$$\xi(Q^2) = \xi + a \ln\left(1 + \frac{Q^2}{Q_0^2}\right),$$

where $a = 0.172$ and $Q_0^2 = 0.265\,{\rm GeV}^2$. Assuming this dependence for higher values of Q^2 and using (30), we then predict saturation of $\lambda(Q^2)$ at large Q^2, i.e. the following flattening should take place:

$$\lambda(Q^2) = a \ln\left(1 + \frac{Q^2}{Q_0^2}\right) \Big/ \left[\xi + a \ln\left(1 + \frac{Q^2}{Q_0^2}\right)\right].$$

The increase of $\xi(Q^2)$ corresponds to the increasing interaction radius of the constituent quarks from the virtual vector meson which is illustrated on Fig. 6.

4 Elastic vector meson production

The calculation of the elastic and inelastic cross sections can also be directly performed similar to the calculation of the total cross-sections using (23), (24) and (25) and integrating the functions $|F^*(s, b, Q^2)|^2$ and $\eta^{**}(s, b, Q^2)$

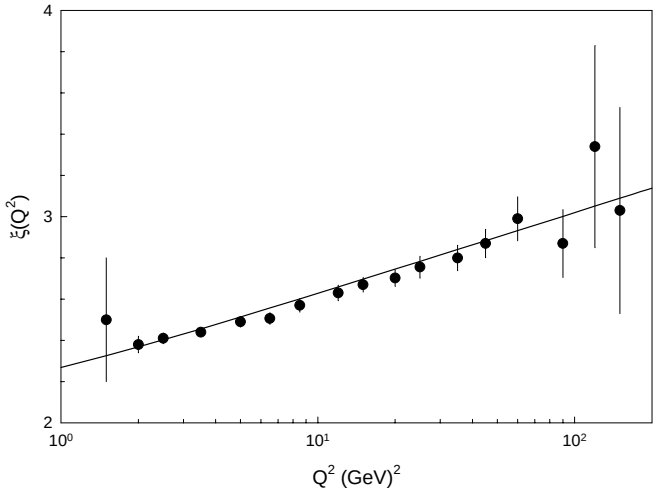

Fig. 5. The "experimental" behavior of the function $\xi(Q^2)$

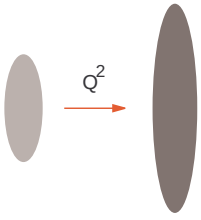

Fig. 6. The increase with virtuality of the constituent quark interaction radius

over the impact parameter. The following asymptotic dependences for the cross sections of elastic scattering and inelastic interactions are obtained in that way:

$$\sigma^{\rm el}_{\gamma^* p}(W^2,Q^2) \propto G_e(Q^2)\left(\frac{W^2}{m_Q^2}\right)^{\lambda(Q^2)} \ln\frac{W^2}{m_Q^2} \qquad (34)$$

and

$$\sigma^{\rm inel}_{\gamma^* p}(W^2,Q^2) \propto G_i(Q^2)\left(\frac{W^2}{m_Q^2}\right)^{\lambda(Q^2)} \ln\frac{W^2}{m_Q^2}, \qquad (35)$$

with the universal exponent $\lambda(Q^2)$ given by (30).

The above relations imply that the ratios of elastic and inelastic cross sections to the total one do not depend on energy. In order to confront these results with experimental data it is useful to keep in mind that, as was noted in [20], diffraction of the virtual photon includes both elastic and inelastic scattering of its fluctuations.

Now we consider elastic (exclusive) cross sections both for the light and heavy vector mesons production. We assumed earlier that the virtual photon before the interaction with the proton fluctuates into a $\bar{Q}Q$-pair and for simplicity we limited ourselves to light quarks in the discussion of the total cross section. Therefore we need to get rid of the light quark limitation and extend the above approach in order to include the quarks with different masses. The inclusion, in particular, of heavy vector meson production into this scheme is straightforward: the virtual photon fluctuates before the interaction with a proton into the heavy quark–antiquark pair which constitutes the virtual heavy vector meson state. After the interaction with a proton this state becomes a real heavy vector meson.

The integral exclusive (elastic) cross section of vector meson production in the process $\gamma^* p \to Vp$ when the final state vector meson contains not only light quarks can be calculated directly according to the above scheme and formulas of Sect. 2:

$$\sigma^V_{\gamma^* p}(W^2,Q^2) \propto G_V(Q^2)\left(\frac{W^2}{m_Q{}^2}\right)^{\lambda_V(Q^2)} \ln\frac{W^2}{m_Q{}^2}, \qquad (36)$$

where

$$\lambda_V(Q^2) = \lambda(Q^2)\frac{\tilde{m}_Q}{\langle m_Q\rangle}. \qquad (37)$$

In (37) $\tilde{m}_Q$ denotes the mass of the constituent quarks from the vector meson and $\langle m_Q\rangle$ is the mean constituent quark mass of the vector meson and proton system. Evidently $\lambda_V(Q^2) = \lambda(Q^2)$ for the light vector mesons. In the case when the vector meson is very heavy, i.e. $\tilde{m}_Q \gg m_Q$, we have

$$\lambda_V(Q^2) = \frac{5}{2}\lambda(Q^2).$$

We conclude that the respective cross section increases faster than the corresponding cross section of the light vector meson production, e.g. (37) results in

$$\lambda_{J/\Psi}(Q^2) \simeq 2\lambda(Q^2).$$

The above results are in a qualitative agreement with the trends observed in the HERA experiments [21,22].

5 Angular structure of elastic vector meson production

Now we turn to a calculation of the scattering amplitudes at $t \neq 0$. This will allow us to get a differential cross section and to confront the results with the first measurements of the angular distributions at large t in light vector meson production [24]. It was found that the angular distribution in the proton dissociative processes [25] is consistent with the power dependence $(-t)^{-3}$. A calculation of the differential cross sections in elastic vector meson production can be performed using the analysis of the singularities of the amplitudes in the complex impact parameter plane which was applied to elastic hadron scattering in [26]. There are different approaches to the vector meson production, e.g. the recent application of the geometrical picture given in [27]. Angular distributions can be described also in the approaches based on the perturbative QCD [28–30] which provides a smooth power-like t-dependence. A brief review of the recent results of these approaches can be found in [31].

Since the integration in the Fourier–Bessel transform goes over the variable b^2 rather than b it is convenient

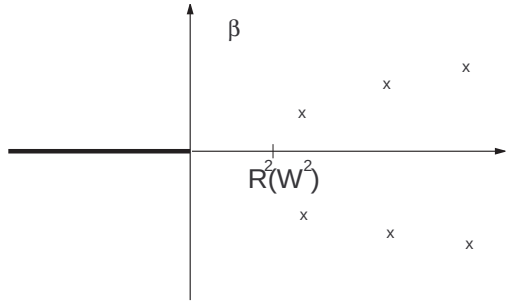

Fig. 7. The singularities of the scattering amplitude in the complex β-plane

to consider the complex plane of the variable β, where $\beta = b^2$, and analyze singularities in β plane. Using (11) we can write down the integral over the contour C around a positive axis in the β plane:

$$F^*(W^2,t,Q^2) = -\mathrm{i}\frac{W^2}{2\pi^2}\int_C F^*(W^2,\beta,Q^2)K_0(\sqrt{t\beta})\mathrm{d}\beta, \tag{38}$$

where K_0 is the modified Bessel function and the variable W^2 was used instead of the variable s. The contour C can be closed at infinity and the value of the integral will then be determined by the singularities of the function $F^*(W^2,\beta,Q^2)$ in the complex β plane (Fig. 7), where

$$F^*(W^2,\beta,Q^2) = \omega(\beta,Q^2)\frac{U(W^2,\beta)}{1-\mathrm{i}U(W^2,\beta)}.$$

With the explicit expressions for the functions U and ω we conclude that the positions of the poles which are determined by solutions of the equation

$$1-\mathrm{i}U(W^2,\beta) = 0$$

are located at

$$\beta_n(W^2) = \left[R(W^2) + \mathrm{i}\frac{\xi}{M}\pi n\right]^2, \quad n = \pm1,\pm3,\dots,$$

where $M = \tilde{m}_Q n_V + m_Q n_h$ and

$$R(W^2) = \frac{\xi}{M}\ln\left[g^N\left(\frac{W^2}{{m_Q}^2}\right)^{N/2}\right].$$

The location of the poles does not depend on the virtuality Q^2.

Besides the poles the function $F^*(W^2,\beta,Q^2)$ has a branching point at $\beta = 0$ and

$$\begin{aligned}&\mathrm{disc}\,F^*(W^2,\beta,Q^2)\\ &= \Big\{\Big(\mathrm{disc}[\omega(\beta,Q^2)U(W^2,\beta)] - \mathrm{i}U(W^2,\beta+\mathrm{i}0)\\ &\quad\times U(W^2,\beta-\mathrm{i}0)\mathrm{disc}\,\omega(\beta,Q^2)\Big)\Big/\Big([1-\mathrm{i}U(W^2,\beta+\mathrm{i}0)]\\ &\quad\times[1-\mathrm{i}U(W^2,\beta-\mathrm{i}0)]\Big)\Big\},\end{aligned}$$

i.e.

$$\mathrm{disc}\,F^*(W^2,\beta,Q^2) \simeq \mathrm{i}\,\mathrm{disc}\,\omega(\beta,Q^2),$$

since at $W^2\to\infty$ the function $U(W^2,\beta)\to\infty$ at fixed β. As a result the function $F^*(W^2,t,Q^2)$ can be represented as a sum of pole and cut contributions, i.e.

$$F^*(W^2,t,Q^2) = F_p^*(W^2,t,Q^2) + F_c^*(W^2,t,Q^2).$$

The pole and cut contributions are decoupled dynamically when $W^2\to\infty$. The contribution of the poles determines the amplitude $F^*(W^2,t,Q^2)$ in the region $|t|/W^2 \ll 1$ and can be written in the form of a series:

$$\begin{aligned}F^*(W^2,t,Q^2) &\simeq \mathrm{i}W^2(W^2)^{\lambda_V(Q^2)/2}\\ &\times\sum_{n=\pm1,\pm3,\dots}\exp\left\{\frac{\mathrm{i}\pi n}{N}\lambda_V(Q^2)\right\}\sqrt{\beta_n}K_0(\sqrt{t\beta_n}).\end{aligned} \tag{39}$$

At moderate values of $-t$ when $-t \geq 1$ $(\mathrm{GeV}/c)^2$ the amplitude (39) leads to the Orear type behavior of the differential cross section which is similar to (32) for the on-shell amplitude, i.e.

$$\frac{\mathrm{d}\sigma_V}{\mathrm{d}t} \propto \exp\left[-\frac{2\pi\xi}{M}\sqrt{-t}\right]. \tag{40}$$

Note that at small t the behavior of the differential cross section is complicated. The oscillating factors

$$\exp\left\{\frac{\mathrm{i}\pi n}{N}\lambda_V(Q^2)\right\},$$

absent in the on-shell scattering amplitude [14], here play a role.

At large t the poles contributions are negligible and the contribution from the cut at $\beta = 0$ is the dominating one. It appears that the function $F_c^*(W^2,t,Q^2)$ does not depend on energy and the differential cross section depends on t in a power-like way,

$$\frac{\mathrm{d}\sigma_V}{\mathrm{d}t} \simeq \tilde{G}(Q^2)\left(1-\frac{\bar{\xi}^2(Q^2)t}{\tilde{m}_Q^2}\right)^{-3}. \tag{41}$$

Therefore for large values of $-t$ $(-t \gg \tilde{m}_Q^2/\bar{\xi}^2(Q^2))$ we have a simple $(-t)^{-3}$ dependence of the differential cross section. This dependence is very distinct from the corresponding behavior of the differential cross section of the on-shell scattering [14] which approximates the quark counting rule [32] due to off-shell unitarity effects. It is worth noting that the ratio of the two differential cross-sections for the production of the vector mesons V_1 and V_2 does not depend on the variables W^2 and t at large values of t.

6 Impact parameter picture

The results described above rely on the off-shell unitarity and the Q^2-dependence of the constituent quark interaction radius. It is useful to consider the impact parameter

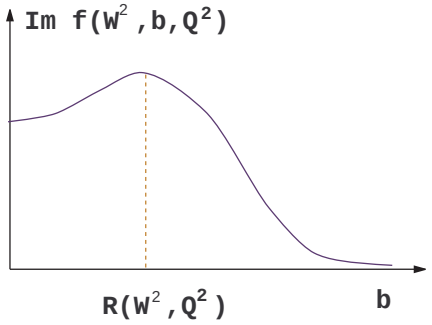

Fig. 8. The impact parameter profile of the scattering amplitude

picture to get insight in the physical origin of this Q^2-dependence. The impact parameter analysis of the experimental data was a particular tool for the detection of the unitarity effects in hadronic reactions [33] and, as was proposed in [20], a similar technique can be used in diffractive DIS. The impact parameter profile of the amplitude is peripheral when $\xi(Q^2)$ increases with Q^2 (Fig. 8). The dependence on the virtuality of the constituent quark interaction radius was assumed and this dependence appeared to be in a qualitative agreement with the experimental data. It was demonstrated then that the increasing dependence of the constituent quark interaction radius with virtuality implies an increasing Q^2-dependence of the exponent $\lambda(Q^2)$. The relation between $\xi(Q^2)$ and $\lambda(Q^2)$ implies in its turn a saturation of the Q^2-dependence of $\lambda(Q^2)$ at large values of Q^2. The reason for the increase of the constituent quark interaction radius with virtuality should have a dynamical nature, and it could originate from the emission of additional $q\bar{q}$-pairs in the non-perturbative structure of a constituent quark. In the present approach the constituent quark consists of a current quark and a cloud of quark–antiquark pairs of different flavors [14]. It was shown that the available experimental data imply a $\ln Q^2$-dependence for the radius of this cloud.

The peripheral profile of the amplitude in its turn can result from the increasing role of the orbital angular momentum of the quark–antiquark cloud when the virtual particles are considered. The generation of a $\bar{q}q$-pairs cloud could be considered in analogy with the theory of superconductivity. It was proposed [34] to push this analogy further and consider an anisotropic extension of the theory of superconductivity which seems to match well the above non-perturbative picture for a constituent quark. The studies [35] of that theory show that the presence of anisotropy leads to axial symmetry of pairing correlations around the anisotropy direction $\hat{\boldsymbol{l}}$ and to particle currents induced by the pairing correlations. In other words, this means that a particle of the condensed fluid is surrounded by a cloud of correlated particles ("hump") which rotate around it with the axis of rotation $\hat{\boldsymbol{l}}$. A calculation of the orbital momentum shows that it is proportional to the density of the correlated particles. The value of the orbital momentum contribution to the spin of the constituent quark can be estimated according to the relation between the contributions of current quarks to the proton spin and the corresponding contributions of current quarks to the spin of the constituent quarks and that of the constituent quarks to the proton spin.

It is evident that the results of the impact parameter analysis are in favor of the increasing role of the orbital angular momenta with virtuality.

7 Conclusion

We considered the limitations the unitarity provides for the $\gamma^* p$ total cross-sections and geometrical effects in the model dependence of $\sigma^{\rm tot}_{\gamma^* p}$. In particular, it was shown that the Q^2-dependent constituent quark interaction radius can lead to a non-trivial, asymptotical result: $\sigma^{\rm tot}_{\gamma^* p} \sim (W^2)^{\lambda(Q^2)}$, where $\lambda(Q^2)$ will be saturated at large values of Q^2. This result is valid when the interaction radius of the virtual constituent quark is increasing with the virtuality Q^2. The data for the structure functions at low values of x continue to demonstrate the increasing total cross-section of $\gamma^* p$ interactions, and therefore we can consider it as a reflection of the increasing with virtuality of the interaction radius of the constituent quark. Thus, we have shown that the power-like parameterization of the experimental data $\sigma^{\rm tot}_{\gamma^* p} \sim (W^2)^{\lambda(Q^2)}$ with Q^2-dependent exponent can have a physical ground and should not be regarded merely as a convenient way to represent the data. Other scenarios which are consistent with unitarity have also been discussed. The general conclusion is that unitarity itself does not lead to a saturation at $x \to 0$, i.e. a slow down of the power-like energy dependence of $\sigma^{\rm tot}_{\gamma^* p}$ and a transition to the energy behavior consistent with the Froissart–Martin bound valid for the on-shell scattering.

In elastic vector meson electroproduction processes the mass and Q^2 dependences of the integral cross section of vector meson production are related to the dependence of the interaction radius of the constituent quark Q on the respective quark mass m_Q and its virtuality Q^2. The behavior of the differential cross sections at large t is to a large extent determined by the off-shell unitarity effects. The smooth power-like dependence on t is predicted. New experimental data would be essential for the discrimination of the model approaches and studies of the interplay between the non-perturbative and perturbative QCD regimes.

Acknowledgements. We are grateful to J.A. Crittenden for communications on the ZEUS experimental data on the angular distributions and A. Borissov for discussions of the HERMES experimental data. We would also like to thank M. Islam, E. Martynov, V. Petrov and A. Prokudin for many interesting discussions of the results.

References

1. A.M. Cooper-Sarkar, R.C.E. Devenish, A. De Roeck, Int. J. Mod. Phys. A **13**, 3385 (1998)
2. C. Lopez, F.J. Yndurain, Phys. Rev. Lett. **44**, 1118 (1980)

3. V.N. Gribov, L.N. Lipatov, Sov. J. Phys. **15**, 438 (1972) 625; L.N. Lipatov, Sov. J. Nucl. Phys. **20**, 94 (1975); Yu.L. Dokshitzer, Sov. Phys. JETP **46**, 641 (1977); G. Altarelli, G. Parisi, Nucl. Phys. B **426**, 298 (1977)
4. L.N. Lipatov, Sov. J. Nucl. Phys. **23**, 338 (1976); E.A. Kuraev, L.N. Lipatov, V.S. Fadin, Sov. Phys. JETP **45**, 199 (1977); Y.Y. Balitsky, L.N. Lipatov, Sov. J. Nucl. Phys. **28**, 822 (1978)
5. P.M. Nadolsky, S.M. Troshin, N.E. Tyurin, Z. Phys. C **69**, 131 (1995)
6. V.A. Petrov, Nucl. Phys. Proc. Suppl. A **54**, 160 (1997); V.A. Petrov, A.V. Prokudin, in Proceedings of the International Conference on Elastic and Diffractive Scattering, Protvino, Russia, 28 June–2 July 1999, p. 95, edited by V.A. Petrov, A.V. Prokudin (World Scientific, 2000)
7. P.V. Landshoff, hep-ph/0010315; A. Donnachie, J. Gravelis, G. Shaw, hep-ph/0101221; S. Munier, A.M. Staśto, A.H. Mueller, hep-ph/0102291
8. C. Adloff et al. [H1 Collaboration], Preprint DESY 01-104, 2001
9. P. Desgrolard, A. Lengyel, E. Martynov, hep-ph/0110149
10. G. Wolf, hep-ex/0105055
11. S.M. Troshin, N.E. Tyurin, Europhys. Lett. **37**, 239 (1997)
12. A.L. Ayala, M.B. Gay Ducati, E.M. Levin, Phys. Lett. B **388**, 188 (1996); A. Capella, E.G. Ferreiro, A.B. Kaidalov, C.A. Salvado, Nucl. Phys. B **593** , 336 (2001)
13. E.A. Paschos, Phys. Lett. B **389**, 383 (1996); W.L. van Neerven, Nucl. Phys. B, Proc. Suppl. **79**, 36 (1999)
14. S.M. Troshin, N.E. Tyurin, Nuovo Cim. A **106**, 327 (1993); Phys. Rev. D **49**, 4427 (1994)
15. R. Blankenbecler, M.L. Goldberger. Phys. Rev. **126**, 766 (1962)
16. A.A. Logunov, M.A. Mestvirishvili, Nguen Van Hieu, O.A. Khrustalev, Nucl. Phys. B **10**, 692 (1969)
17. T.T. Chou, C.N. Yang, Phys. Rev. **170**, 1591 (1968)
18. O.A. Khrustalev, V.I. Savrin, N.E. Tyurin, Comm. JINR E2-4479, 1969
19. A.M. Staśto, K. Golec-Biernat, J. Kwieciński, hep-ph/0007192; J. Bartels, H. Kowalski, hep-ph/0010345
20. B. Povh, B.Z. Kopeliovich, E. Predazzi, Phys. Lett. B **405**, 361 (1997)
21. ZEUS Collaboration, J. Breitweg et al., Paper 439 submitted to the XXXth International Conference on High Energy Physics, July 27–August 2, 2000, Osaka, Japan
22. R. Ioshida, hep-ph/0102262 and references therein
23. C. Lovelace, Phys. Rev. B **135**, 1225 (1964)
24. ZEUS Collaboration, J. Breitweg et al., Paper 442 submitted to the XXX International Conference on High Energy Physics, 27 July–2 August, 2000, Osaka, Japan
25. J.A. Crittenden, hep-ex/0010079, references therein and private communication
26. S.M. Troshin, N.E. Tyurin, Theor. Math. Phys. **50**, 150 (1982)
27. A.C. Caldwell, M.S. Soares, hep-ph/0101085
28. D.Yu. Ivanov, Phys. Rev. D **53**, 3564 (1996); D.Yu. Ivanov, R. Kirschner, A. Schaäfer, L. Szymanowski, Phys. Lett, B **478**, 101 (2000)
29. J.R. Forshaw, G. Poludniowski, hep-ph/0107068
30. E. Gotsman, E. Levin, U. Maor, E. Naftali, TAUP 2691/2001, hep-ph/0110256
31. M. Diehl, hep-ph/0109040
32. V.A. Matveev, R.M. Muradyan, A.N. Tavkhelidze, Lett. Nuovo Cim. **7**, 719 (1973); S. Brodsky, G. Farrar, Phys. Rev. Lett. **31**, 1153 (1973)
33. U. Amaldi, K.R. Schubert, Nucl. Phys. B **166**, 301 (1980)
34. S.M. Troshin, N.E. Tyurin, Phys. Rev. D **52**, 3862 (1995); ibid. D **54**, 838 (1996); Phys. Lett. B **355**, 543 (1995)
35. P.W. Anderson, P. Morel, Phys. Rev. **123**, 1911 (1961); F. Gaitan, Annals of Phys. **235**, 390 (1994); G.E. Volovik, Pisma v ZhETF, **61**, 935 (1995)